Rotor Fault Detection in Squirrel Cage Induction Motors using MCSA and DWT Techniques

Noureddine Bessous, Salim Sbaa, Remus Pusca, Raphaël Romary

Rotor Fault Detection in Squirrel Cage Induction Motors using MCSA and DWT Techniques

Noureddine BESSOUS[(1)*], Salim SBAA[(2)], Remus PUSCA[(3)], Raphaël ROMARY[(3)]
[(1)] Department of electrical engineering, University of El-Oued, El-Oued, Algeria
[(2)] Department of electrical engineering, University of Mohammed Khider, Biskra, Algeria
[(3)] Laboratory of Electrotechnical and Environmental Systems (LSEE), University of Artois, Béthune, France
[*]nbessous@yahoo.fr

Abstract: This article presents the fault detection of broken rotor bar (BRB) faults in squirrel cage induction motors (SCIMs). This work applied two diagnostic methods on stator current signal. It is necessary to verify the machine health to avoid any catastrophic damage. The first method uses the fast Fourier transform (FFT) which is generally called motor current signature analysis (MCSA). We carefully verified the spectral content of the stator current to detect BRB fault. The new harmonics allows us to take a good decision about BRB fault. The second method is based on the discrete wavelet transform (DWT). This technique is widely used in the diagnosis field of rotating machinery. According to DWT method, we used the mean square error (MSE) as a good indicator. An experimental test with different conditions of the induction motor has been performed. The experimental results have been exploited using MCSA and DWT methods to achieve a good decision.

Keywords: Broken rotor bar faults, Discrete wavelet transform, Motor current signature analysis, Discrete wavelet transform

1. INTRODUCTION

In the industry sector, the squirrel cage induction motor (SCIM) is widely used. It has many advantages as robust, self-starting, and facilitates to keep a constant speed (in low load to full load), set by the frequency of the power supply and the number of poles of the stator winding. For this, it used almost 95% of the induction motors in the industry. However, faults in SCIMs can be classified as:

- Stator faults such as: magnetic circuit fault, short circuit of the coils, opening of a phase, stator eccentricity, etc. [1-2].
- Rotor faults such as: rotor eccentricity, bearing problem, BRB faults, etc. [3-4].

Generally, faults produce many similar symptoms as unbalanced voltages or electric currents, air-gap variation, decreased average torque, increased losses in efficiency, increased torque pulsations, excessive heating, etc.

The variation of the air-gap value affect on the electromagnetic field distributions which creates new sidebands harmonics in the stator current spectra [5,7]. The verification of some sideband frequencies can be used as a good indicator to BRB faults detection.

Researchers have used many success methods as the FFT that is applied on vibration signal, stator current signal, electromagnetic torque signal, speed signal, etc. to detect different faults in the rotating electrical machines [8,12]. Other techniques have been used to detect the BRB faults in IMs as motor vibration signature analysis (MVSA), wavelet transforms, fuzzy logic, artificial neural network (ANN), and motor current signature analysis by FFT (MCSA-FFT), etc. [13], [17-19].

MCSA-FFT has benefits; but it has some disadvantages as limitations in no-stationary regime.

This study will try to do a very detailed check about the characteristic frequencies for the BRB faults. It is based on the experimental data exploitation.

On the other hand, advanced signal processing techniques as Continuous and/or Discrete Wavelet Transform (CWT, DWT), Wavelet Packet Transform (WPT), Hilbert Transform (HT), Empirical Mode Decomposition (EMD), etc. have been used to detect many faults in SCIMs [20-21].

In this work, DWT is used with the definition of a new estimator which is called mean square error (MSE).

Experimental results help us to measure the stator current signal under different conditions. This study will try to compare the effectiveness between MCSA-FFT and DWT methods.

2. MOTOR TEST BENCH

We used a SCIM with the characteristic as follow: 3kW, f_s=50Hz, 2-pole, 28 bars (Fig.1).

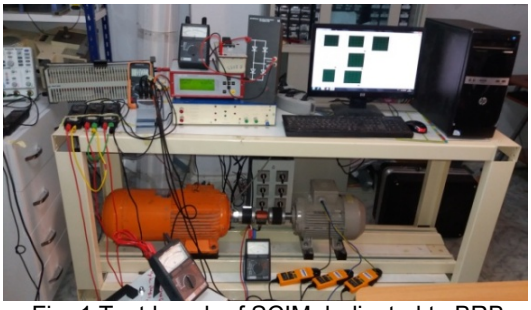

Fig. 1 Test bench of SCIM dedicated to BRB faults.

Fig. 2 presents the photos of rotor SCIM (healthy and faulty).

Fig. 2 Rotors photos (healthy and faulty rotor).

3. BROKEN ROTOR BARS DETECTION USING MCSA-FFT

Generally, SCIM under BRB faults appear in the stator current spectral content as the sideband components. The additional harmonics can be expressed by [5]:

$$f_{BRBs} = (1 \pm 2ks).f_s \qquad (1)$$

where, k=1,2,3, ..., s is the slip of the induction motors.

According to [22-23], other harmonics can be appeared in the stator current spectrum as:

$$f_{BRBs} = \left[(6k \pm 1) \pm 2ks\right] f_s \qquad (2)$$

where, k=1,2,3, ...,

The orders: 5, 7, 11, 17, 19, 23, 25 … (6*k*±1) have the harmonics: (6k±1)×f_s.

The last formula shows other frequencies which is called sideband frequencies (SBFs).

In addition, it's known that these harmonics are introduced in magneto-motive force (FMM). They vary in presence of the BRB faults and/or the slip variation.
The stator current harmonics (6k±1)×f_s are modulated in amplitude at the frequency 2×(6k±1)×sf_s.
Other harmonic series can be found under BRB faults, they are given by:

$$f_{BRBs} = \left[\frac{k}{p}(1-s) \pm s\right].f_s \qquad (3)$$

with, (*k*/*p*=1, 5, 7, 11,…)

As mixed eccentricity of the rotor is always present, the additional frequencies caused by the mixed eccentricity are given by:

$$f_{mix-ecc} = \left|f_s \pm kf_r\right| \qquad (4)$$

where, k=1,2,3, ...

a. 0% of the load operation of SCIM

Fig. 3 presents the stator current spectrum under 0% of the load (s≈0). Due to the slip value which is close to zero (s≈0), the additional frequencies are not found. It's clear that difficult to detect the BRB faults at no load using the MCSA-FFT method.

Among the frequencies because the mixed eccentricity of the rotor are: $f_{mix\text{-}ecc(-)}$ =25.1 Hz and $f_{mix\text{-}ecc(+)}$= 74.9 Hz.

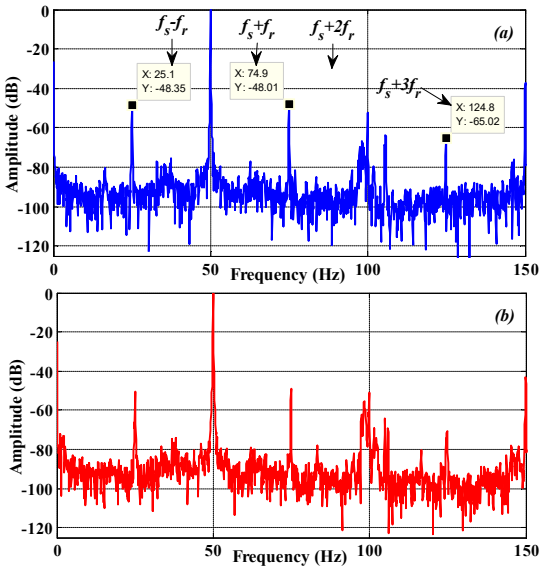

Fig. 3 Stator current spectrum (0-150Hz)

Fig. 4 shows the frequencies around 250Hz and 350Hz.

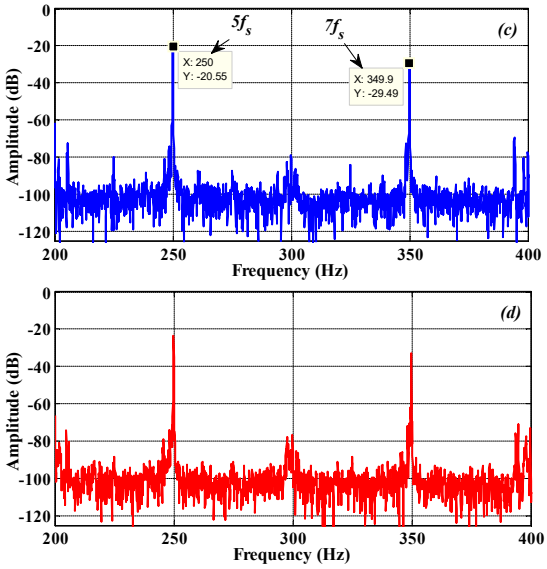

Fig. 4 Stator current spectrum (200-400Hz).

We notice that the additional frequencies caused by BRB faults are almost invisible.

For example, we found $2\times s\times f_s = 0$ (s = 0). In this case the characteristic frequencies of the BRB faults will be invisible.

2- 75% of the load operation of SCIM

In this part, we apply a resistant torque which gives a load of 75% (i.e. s = 3.6%).
It's clear that the BRB faults induce the additional SBFs around the fundamental (f_s) and the harmonics 5, 7 and the *RSHs*.
The SBFs presented in Fig. 5 and showed that the frequencies move with the slip value.
Table I resume the additional harmonics around the supply frequency, 5, 7, and *RSHs*.

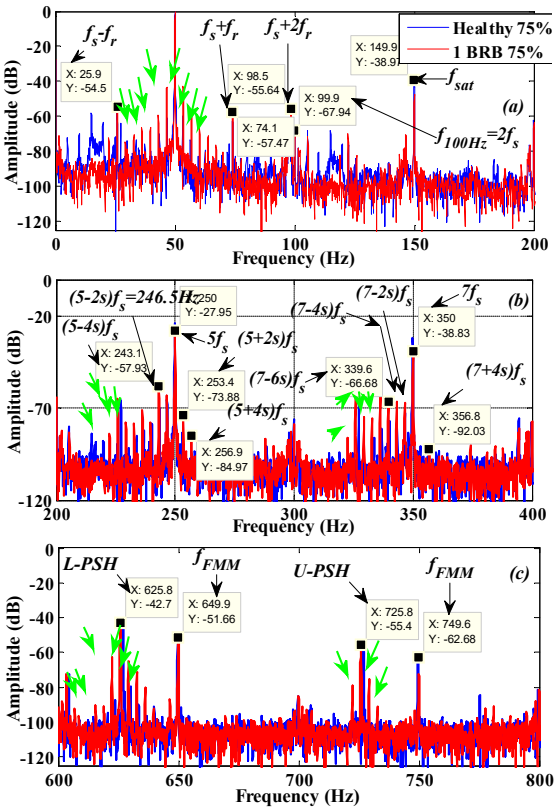

Fig. 5 Stator current spectrum (a): 0-200 Hz, (b): 200-400 Hz, (c): 600-800 Hz.

The SBF values verify the formula (1) (Fig. 6-a). Other SBFs around the rotor slot harmonics (*RSHs*) were verified in Fig. (6-c). These frequencies are attached with RSHs and spaced by $2\times s\times f_s$; we can conclude to the following formula:

$$f_{BRB-RSHs} = RSH \pm 2ksf_s \qquad (5)$$

Some mixed eccentricity frequency components which are always exist in the stator spectrum (healthy or faulty) as f_s-f_r, f_s+f_r, f_s+2f_r, etc.
In addition, saturation frequencies (f_{sat}) are appeared on the spectrum of experimental results. They have the formula as follows:

$$f_{sat} = 3kf_s \qquad (6)$$

where, k is an odd number.

The double component of the supply frequency f_{doub}=100 Hz is appeared clearly:

$$f_{doub-s} = f_{100Hz} = 2f_s \qquad (7)$$

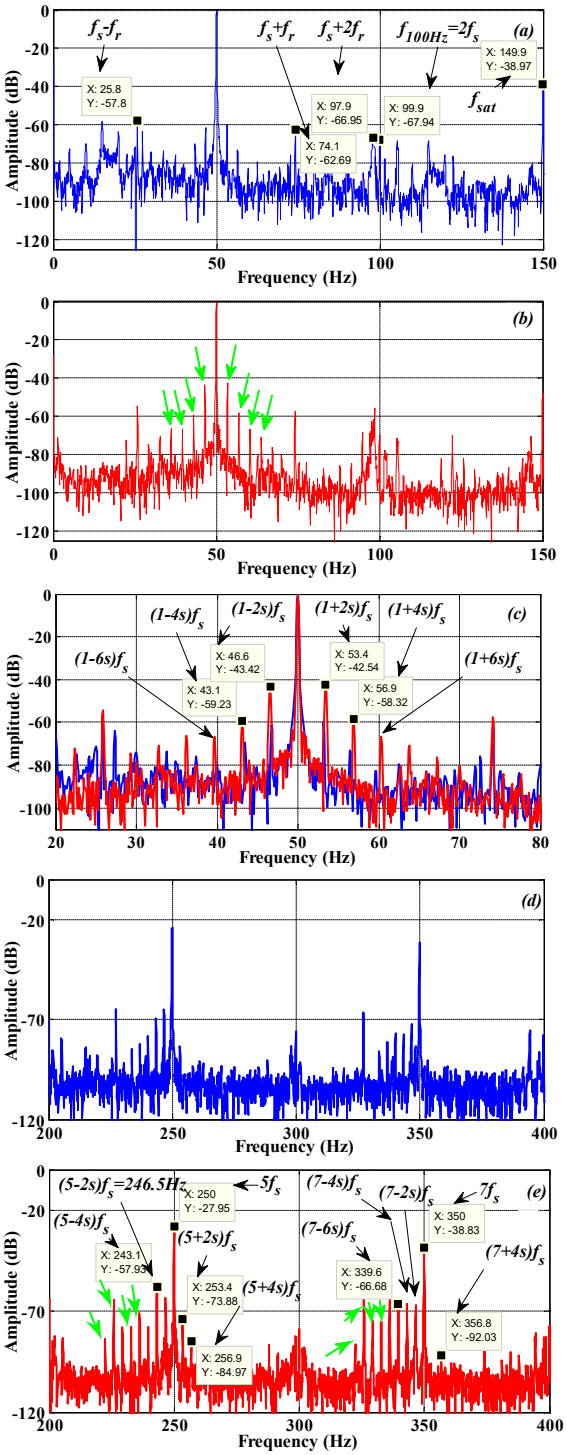

Fig. 6 Stator current spectrum at 75% of load; (a), (b), (c): Around f_s and (d), (e): Around 5, 7.

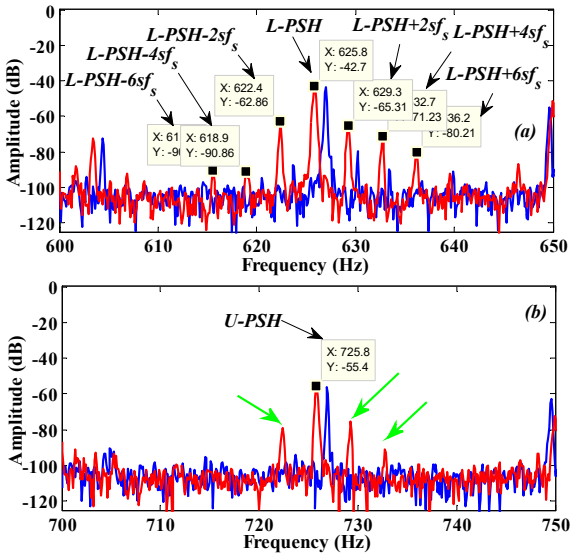

Fig. 7 Stator current spectrum at 75% of load; (a): Around *L-PSH* and (b): Around *U-PSH*.

Table 1: Harmonics of the stator current spectrum (1BRB)

Formulas of characteristic frequencies	Theoretical values (Hz)	Experimental values (Hz)	Amplitude «healthy» (dB)	Amplitude « 1BRB » (dB)
(1-2s)f_s	46.4	46.6	-61.7	**-43.42**
(1+2s)f_s	53.6	53.4	-59.67	**-42.54**
5f_s	250	250	-23.91	**-27.95**
(5-2s)f_s	246.4	246.5	-65.15	**-63.36**
(5+2s)f_s	253.6	253.4	-83.2	**-73.88**
7f_s	350	350	-31.51	**-38.83**
$RSH_1^{(-)} - 2sf_s$	621.2	622.4	-87.38	**-62.86**
$RSH_1^{(-)} + 2sf_s$	628.4	629.3	-79.64	**-65.31**

After this section, we can conclude to these points:

- At no-load operation, it's difficult to found the additional frequencies under BRB faults
- It's clearly in Fig. (5) and Fig. (6) the existence of SBFs in the healthy state of the IM which characterize the BRBs.

4. DETECTION OF BRB FAULTS USING DWT

The section is based on an analysis of the stator current using discrete wavelet transform (DWT).

DWT based on a successive operation from a high-pass filter (HP), and low pass filter (LP) which leads to find the approximation (a_i) and details (d_i). Each step is conducted to the first level. One of two results is the approximation *a1* and the other

is the detail *d1*. *a1* is the approximate shape of the original signal without noise, and *d1* is the detailed shape of the signal that influences on original signal (noise).
Fig. 8 shows the discrete wavelet transform scheme.

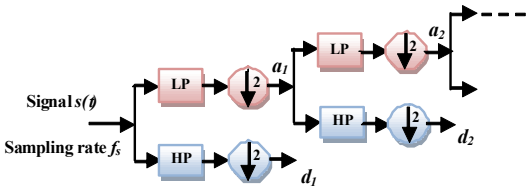

Fig. 8 Discrete wavelet decomposition scheme.

These decompositions are limited by the number N_{LL}:

$$N_{LL} = \text{int}\left[\frac{\log\left(\frac{f_{sa}}{f_s}\right)}{\log(2)}\right]$$

f_{sa}=12.8Hz, f_s=50Hz are the sampling frequency used for experimental recovery and fundamental frequency respectively.

[24,25] have many detailed about the choice of the mother wavelet and the adequate number for decomposition levels.

The level numbers (N_{LN}) of decomposition, advisable is:

$$N_{LN} = \text{int}\left[\frac{\log\left(\frac{12.8\times10^3}{50}\right)}{\log(2)}\right] + 1 \; or \; 2 = 9 \; or \; 10 \; levels$$

According to Shannon's theorem, the frequency details are included in the following bands:

$$f_{di} \in \left[\left(\frac{f_{sa}}{2^{(i+1)}}\right) \rightarrow \left(\frac{f_{sa}}{2^{i}}\right)\right] \; Hz$$

The bands frequencies of the approximations signals a_j are the following:

$$f_{aj} \in \left[0 \rightarrow \left(\frac{f_{sa}}{2^{(j+1)}}\right)\right] \; Hz$$

Table (II) indicates to the different frequency bands:

Table II. Frequency bands of levels

Frequency bands of level decomposition (Hz)	
d_7	50 - 100
d_8	25 - 50
d_9	12.5 - 25

We used the mother wavelet Daubechies 44 (db 44) to the decomposition into multi-level of the stator current sgnal.

Fig. (9) and Fig. (10) show the DWT decomposition of the stator current in healthy and faulty state under different load operation(0% and 75%). The figures show the details : d1 to d9 and the approximation a9

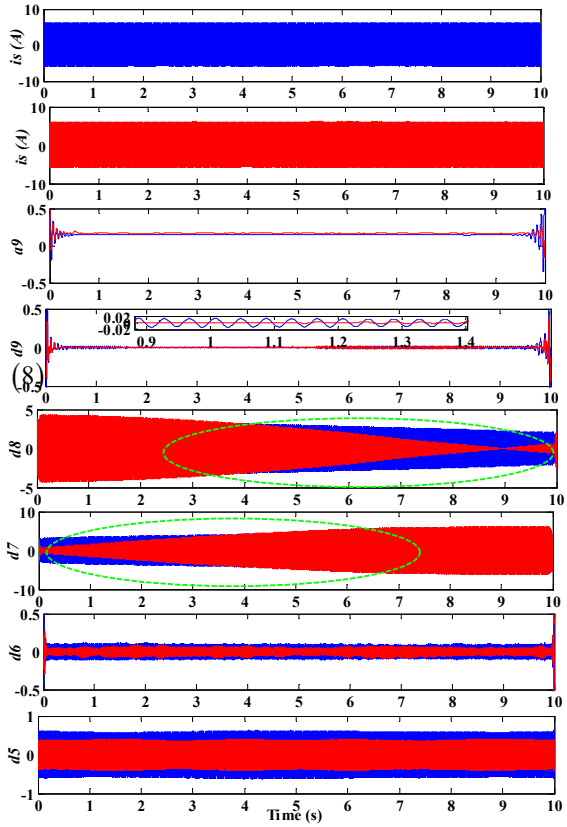

(8)

Figure 9. DWT analysis of stator current at 0% of the load (healthy: blue; 1BRB: red)

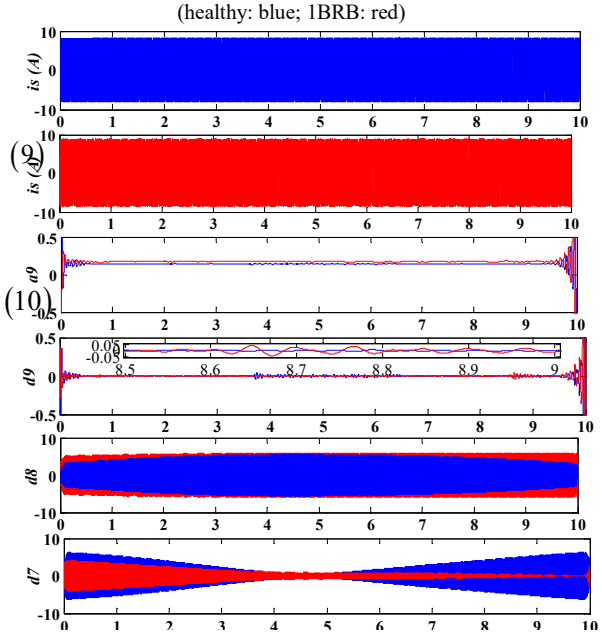

(9)

(10)

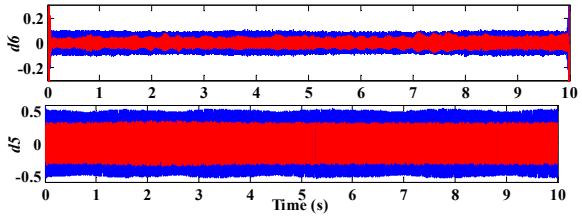

Fig. 10 DWT analysis of stator current at 75% of the load (healthy: blue; 1BRB: red).

The signal evolution of different conditions is well presented on Fig. (9) and Fig. (10), especially in details d5 to d9 and the approximation a9. The frequency bands affected are:

d_5	200 - 400
d_6	100 - 200
d_7	50 - 100
d_8	25 - 50
d_9	12.5- 25

a. Details Energy

We can calculate the energy of each detail as follows:

$$E_j = \sum_{n=1}^{N} \left| d_j(n) \right|^2 \qquad (11)$$

Where j is the level of detail, d_j is the detail signal at level j and N is the total number of samples in the signal.

Fig. 11 and Fig. 12 show the variation of the energy for two conditions of the induction motors. The difference between the energies is clearly appeared. The information of BRB fault is revealed and the energy variation of *d7* is remarkable. There are a changed in the energies of d5 and d8 also.

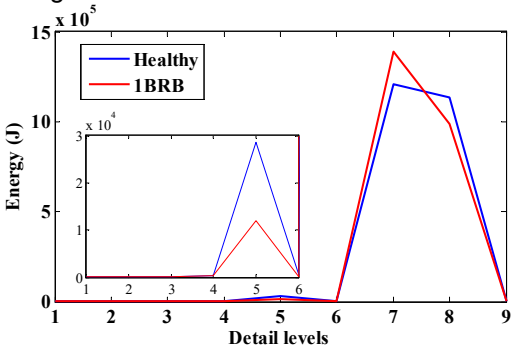

Fig. 11 Energy level from 1 to 9 of stator current at 0% of the load.

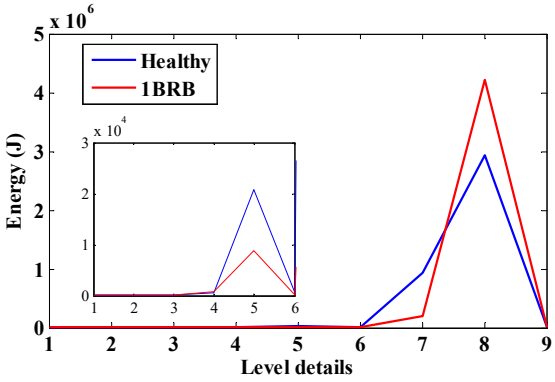

Fig. 12 Energy level from 1 to 9 of stator current at 75% of the load.

This comparison allows us to verify how the frequency responsible bandwidth energy level. We can stop at *d6* to show the difference and to find the fault information.

b. Mean Square Error 'MSE'

MSE can be used as a quality and/or quantity indicator by a percentage of correspondence between the signals.

MSE is a frequently measure used to verify the difference between the values predicted by a model in the healthy state and the values of faulty state [26].

The resemblance coefficient of MSE for two signals X_1 and X_2 (in each position i) which have a point numbers n is calculated by:

$$MSE = \frac{\sum_{i=1}^{n} (X_{1,i} - X_{2,i})^2}{n} \qquad (12)$$

We have used this indicator the details di to determine the frequency band. On the other hand is to determine the dominant detail in the new signal.

The resemblance of the signals is checked for MSE value that tends to zero.

Details and approximations provide much information on the existence of the BRB faults.

The figures below show the qualitative and quantitative aspects of our analysis by the MSE values.

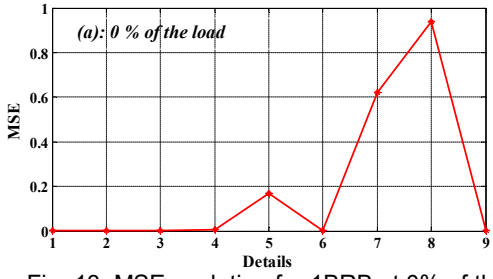

Fig. 13. MSE evolution for 1BRB at 0% of the load.

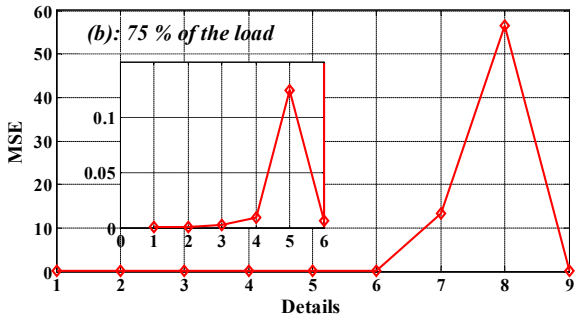

Fig. 14. MSE evolution for 1BRB at 75% of the load.

The DWT analysis is a very effective tool for the BRB fault detection. Precisely, the introduction of the MSE gave well information about the BRB fault exists.

It has been noticed that the most significantly affected bands for this BRB fault analysis are 25 Hz to 100 Hz (d7 and d8). This frequency band shows the effect of the SBFs around the fundamental frequency which have been found by the FFT method.

5. CONCLUSION

The FFT was used on the stator current signal to find the harmonic contents.

MCSA-FFT technique shows a good correspondence with the literature studies as harmonic displacement, frequency values, and the severity degree of the BRB faults.

It is important to notice that the presence or absence of the characteristic frequencies is dependent on the operating mode (at no-load or load motor). In addition, it is difficult to detect the BRB fault using MCSA at no-load operation. On the other hand, this method is not valid in the non-stationary regime.

DWT analysis has been used on the stator current signal. According to the results, the information about BRB fault is clear (d7 and d8). MSE value gave quantitative and qualitative terms in section (4.b).

After this study, the stator current analysis using DWT method is adequate to detect the BRB faults. DWT is sensitive to any change in the stator current signal as it is effective for both operation regimes: stationary and non-stationary.

We can advice in the future study to other indicators as: Root Mean Square Error (RMSE) and Normalized Mean Square Error (NMSE) to find a good indicator.

References

[1] A. M. Júnior, V.V. Silva, L.M. Baccarini, L.F.Mendes, “The Design of Multiple Linear Regression Models using a Genetic Algorithm to diagnose Initial Short-Circuit Faults in 3-Phase Induction Motors,” *Applied Soft Computing*, pp. 50-58, 2018.

[2] H. H. Eldeeb, H. Zhao, O. Mohammed, “Effect of Stator's Insulation Failure on the Performance of Motor Drive system,” *IEEE International Applied Computational Electromagnetics Society Symposium (ACES)*, pp. 1-2, 2020.

[3] G. Singh, V. N. A. Naikan., “Detection of Half Broken Rotor Bar Fault in VFD Driven Induction Motor Drive using Motor Square Current MUSIC Analysis,” *Mechanical Systems and Signal Processing*, pp. 333-348, 2018.

[4] N. Bessous, S.E. Zouzou, S. Sbaa, W.Bentrah, Z. Becer, R. Ajgou, “Static Eccentricity Fault Detection of Induction Motors using MVSA, MCSA and Discrete Wavelet Transform (DWT),” *in Electrical Engineering Conference -Boumerdes (ICEE-B)*, *IEEE*, 2017, pp. 1-10.

[5] F. Filippetti, F., M. Martelli, G. Franceschini, C. Tassoni., “Development of Expert System Knowledge Base to On-Line Diagnosis of Rotor Electrical Faults of Induction Motors,” *in Industry Applications Society Annual Meeting Conference*, *IEEE*, 1992 pp. 92-99.

[6] N. Bessous, S.E. Zouzou, S. Sbaa, A. Khelil, “New Vision about the Overlap Frequencies in the MCSA-FFT Technique to Diagnose the Eccentricity Fault in The Induction Motors,” *in Electrical Engineering Conference*, *IEEE*, 2017, pp. 1-6.

[7] M. Deeb, N.F. Kotelenets, “Fault Diagnosis of 3-phase Induction Machine Using Harmonic Content of Stator Current Spectrum,” *IEEE International Youth Conference on Radio Electronics, Electrical and Power Engineering (REEPE)*, pp. 1-6, 2020.

[8] N. Bessous, S. E. Zouzou, S. Sbaa, W. Bentrah., “A Comparative Study between the MCSA, DWT and the Vibration Analysis Methods to Diagnose the Dynamic Eccentricity Fault in Induction Motors,” *in Systems and Control Conference (ICSC)*, *IEEE*, 2017, pp. 414-421.

[9] Y. Hu, C. Fangsen, X. Tu, F. Li, “Bayesian estimation of instantaneous speed for rotating machinery fault diagnosis,” IEEE Transactions on Industrial Electronics, 2020.

[10] J. Martinez, A. Belahcen, A. Muetze, “Analysis of the Vibration Magnitude of an Induction Motor with Different Numbers of Broken Bars,” *IEEE transactions on industry applications*, pp. 2711-2720, 2017.

[11] M. Akar, H.S. Gercekcioglu, “Instantaneous Power Factor Signature Analysis for Efficient Fault Diagnosis in Inverter Fed Three Phased Induction Motors,” *International Journal of Hydrogen Energy*, pp. 8338-8345, 2017.

[12] M. Dybkowski, K. Klimkowski, “Speed Sensor Fault Detection Algorithm for Vector Control Methods Based on the Parity Relations,” *in Power Electronics and Applications Conference*, *IEEE*, 2017, pp. P-1.

[13] M. Mohamed, E. Mohamed, A.A. Mohamed, M. Abdel-Nasser, M.M. Hassan, “Detection of Inter Turn Short Circuit Faults in Induction Motor using Artificial Neural Network,” *The 26th Conference of Open Innovations*

Association (FRUCT), IEEE, pp. 297-304, 2020.

[14] S. S. Shetgaonkar, "Fault Diagnosis in Induction Motor using Fuzzy Logic," *in Computing Methodologies and Communication Conference (ICCMC)*, *IEEE*, 2017, pp. 289-293.

[15] G. H. Bazan, P.R. Scalassara, W. Endo, A. Goedtel, W.F. Godoy, R.H.C. Palácios, "Stator Fault Analysis of Three-Phase Induction Motors using Information Measures and Artificial Neural Networks," *Electric Power Systems Research*, pp. 347-356, 2017.

[16] H.D. Rações, F.J. Ferreira, J.M. Pires, C.V. Damásio, "Application of Different Machine Learning Strategies for Current-and Vibration-based Motor Bearing Fault Detection in Induction Motors," *In IECON 2019-45th Annual Conference of the IEEE Industrial Electronics Society*, pp. 68-73, 2019.

[17] N. Bessous, A. Chemsa, S. Sbaa, S., "December. New Vision about the Mixed Eccentricity Fault Causes in Induction Motors and its relationship with the Rolling Element Bearing Faults: Analytical model dedicated to the REB faults," *IEEE International Conference on Communications and Elec trical Engineering (ICCEE)*, pp. 1-11, 2018.

[18] Y. Park, M. Jeong, S.B. Lee, J.A. Antonino-Daviu, M.Teska, "Influence of Blade Pass Frequency Vibrations on MCSA-Based Rotor Fault Detection of Induction Motors," *IEEE Transactions on Industry Applications*, pp. 2049-2058, 2017.

[19] N. G. Lo, A. Soualhi, , M.Frinì, H., Razik, "Gear and Bearings Fault Detection using Motor Current Signature Analysis," *in Industrial Electronics and Applications Conference*, *IEEE*, 2018.

[20] A. Mejia-Barron, M. Valtierra-Rodriguez, D. Granados-Lieberman, J.C. Olivares-Galvan, R. Escarela-Perez, "The Application of EMD-Based Methods for Diagnosis of Winding Faults in a Transformer using Transient and Steady State Currents," *Measurement*, pp. 371-379, 2018.

[21] P. S. Panigrahy, P. Konar, P. Chattopadhyay, "Broken Bar Fault Detection using Fused DWT-FFT in FPGA Platform," *in Power, Control and Embedded Systems Conference (ICPCES)*, *IEEE*, pp. 1-6, 2014.

[22] W. Deleroi, "Broken Bar in Squirrel Cage Rotor of an Induction Motor, Pan I: Description by Superimposed Fault Currents," *Arch. fur Elektrotechnik*, pp. 91-99, 1984.

[23] L. Abdesselam, G. Clerc, "Study of Rotor Asymmetry Effects of an Induction Machine by Finite Element Method," *Journal of Electrical Engineering and Technology*, pp. 342-349, 2011.

[24] J. A., Antonino-Daviu, M. Riera-Guasp, J. R. Folch, M. P. M. Palomares, "Validation of a New Method for the Diagnosis of Rotor Bar Failures Via Wavelet Transform in Industrial Induction Machines," *IEEE Transactions on Industry Applications*, pp. 990-996, 2006.

[25] N. Bessous, S. E. Zouzou, W. Bentrah, S. Sbaa, M. Sahraoui, "Diagnosis of Bearing Defects in Induction Motors using Discrete Wavelet Transform," *International Journal of System Assurance Engineering and Management*, pp. 335-343, 2018.

[26] N. Bessous, S. Sbaa, S.E. Zouzou, W. Bentrah, Z. Becer, L. Zarour, "Application of New Quantitative and Qualitative Study Based on DWT Method To Diagnose the Eccentricity Fault in Induction Motors," *in Electrical Engineering Conference (ICEE-B)*, *IEEE*, 2017, pp. 1-6.